

Coherent Dynamics of a Josephson Charge Qubit

T. Duty,¹ D. Gunnarsson,¹ K. Bladh,¹ R. J. Schoelkopf,² and P. Delsing¹

¹Microtechnology and Nanoscience, M C 2, Chalmers University of Technology, S-412 96 Goteborg, Sweden

²Departments of Applied Physics and Physics, Yale University, New Haven, CT 06511 USA

(Dated: May 10, 2003)

We have fabricated a Josephson charge qubit by capacitively coupling a single-Cooper-pair box (SCB) to an electrometer based upon a single-electron transistor configured for radio-frequency readout (RF-SET). Charge quantization of $2e$ is observed and microwave spectroscopy is used to extract the Josephson and charging energies of the box. We demonstrate coherent manipulation of the SCB by using very fast DC pulses, and observe quantum oscillations in time of the charge that persist to a few ns. Initial oscillation amplitudes as high as 0.5e are observed, with the reduction from the maximum of $1.0e$ being understood as an adiabatic effect of the finite risetime of the pulses.

Although a large number of physical systems have been suggested as potential implementations of qubits, solid state systems are attractive in that they offer a realistic possibility of scaling to a large number of interacting qubits. Recently there has been considerable experimental progress using superconducting microelectronic circuits to construct artificial two-level systems. A variety of relative Josephson and Coulomb energy scales have been used to construct qubits based upon a single-Cooper-pair box [1, 2] and flux qubits based upon a 3-junction loop [3, 4]. Coherence times of the order of 0.5 microseconds have been achieved for a single-Cooper-pair box qubit [2]. Rabi oscillations between energy levels of a single large tunnel junction have also been observed [5, 6].

The experimental systems reported so far can also be distinguished by the readout method, and the manner of performing single qubit rotations. The first demonstration of coherent control of a single-Cooper-pair box (SCB) [1] employed a weakly coupled probe junction to determine the charge on the island. In the more recent experiment reported by Vion et al. [2], the SCB was incorporated into a loop containing a large tunnel junction, for which the switching current depends on the state of the SCB. Switching current measurements of SQUIDS have also been used for flux and phase-type qubits [3, 4, 5, 6]. Nakamura et al. [1] performed single qubit rotations by applying very fast DC pulses to a gate lead in order to quickly move the SCB into, and away from the charge degeneracy point. This technique produces ≈ 2 qubit rotations with an operation time that can be of the order of the natural oscillation period. Other experiments have opted to utilize microwave pulses to perform NMR-like rotations of the qubit [2, 4, 5, 6]. The latter approach requires less stringent microwave engineering, since RF-rotations can be accomplished with pulses that are at least an order of magnitude slower in rise time and duration than the natural oscillation period but has the disadvantage of an increased single qubit operation time.

In this letter, we report measurements made on a SCB-type qubit with very fast DC pulses used to effect the qubit rotations as in Nakamura et al. [1]. For our qubit,

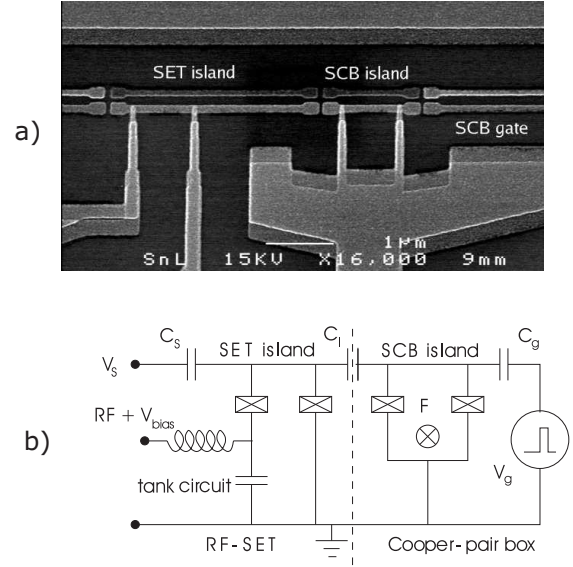


FIG. 1: (a) Scanning electron micrograph of sample 1. The device consists of a Cooper-pair box and SET electrometer and was fabricated by double-angle shadow evaporation of an aluminum film (lighter regions) onto an oxidized Si substrate (darker regions), using oxidation between the first and second layers to create the tunnel junctions. (b) Circuit diagram of box and electrometer.

however, the readout system consists of a single-electron-transistor (SET) capacitively coupled to the SCB, and configured for radio-frequency readout (RF-SET) [7]. By incorporating a SET into a tank circuit, RF-SET electrometers can be made that are both fast and sensitive [8], and are well-suited for SCB-qubit readout [9, 10]. The advantage of using RF-SET readout is that it can easily be turned on and off, although for the measurements reported here it is operated in a continuous mode that weakly measures the charge on the SCB as reported in a previous experiment [10].

Electron beam lithography and double-angle shadow evaporation of aluminum films onto an oxidized silicon substrate were used to fabricate the combined SCB-SET system [Fig. 1] [11]. The SCB box consists of a low-

capacitance superconducting island connected to a superconducting reservoir by two parallel junctions that define a low-inductance SQUID loop. An additional gate lead placed near the island is used to change the electrostatic potential of the island by a gate voltage V_g through a gate capacitance C_g . By adjusting the magnetic flux through the loop, the effective Josephson energy is tunable as $E_J = E_J^{\max} \cos(\phi = \phi_0)$, where ϕ_0 is the magnetic flux quantum ($\hbar=2e$). Coupling of the SCB to the SET was accomplished by extending part of the SET island to the proximity of the box island and resulted in a weak dimensionless coupling, $C_I = C$ of 2–4% for samples with slightly different geometries. C_I is the capacitance between the SCB and SET islands and C is the total capacitance of the SCB.

The samples were placed at the mixing chamber of a dilution refrigerator with a base temperature of approximately 20 mK. A superconducting magnet was used to produce a field nearly parallel to the plane of the samples. This allowed us to both suppress the superconducting gap of the aluminum film, and change the effective Josephson energy of the Cooper-pair box. All control lines were filtered by a combination of low-pass and stainless steel and copper-powder filters. In order to present sharp pulses to the SCB gate, however, only 10 dB attenuation at 4.2 K and 20 dB at room temperature was used for the high frequency coaxial line.

The tank circuit was found to have a resonant frequency of 380 MHz, and the RF-SET electrometer was biased near a feature in the IV versus V_g^{SET} landscape known as the double Josephson quasiparticle peak (DJQP) [12], such that the bias current through the SET was typically 200–300 pA. Under these conditions, the electrometer sensitivity for the combined SCB-SET system was found to be 50 μeV Hz with a bandwidth of 10 MHz.

To make an artificial two-level system, the energy scales of the SCB must be chosen so that $k_B T \ll E_C$, where E_C is the energy cost required to add a single electron to the island and is set by total capacitance of the island $E_C = e^2/2C$. If C is large enough compared to E_C , then the low energy states will be even parity states that differ only by the average number of Cooper-pairs on the island. The effective Hamiltonian of the box, including the Josephson coupling, is given by

$$H = 4E_C \sum_n (n - n_g)^2 \hat{n}_n \hat{n}_j + \frac{E_J}{2} \sum_n (\hat{n}_{j+1} \hat{n}_j + \hat{n}_j \hat{n}_{j+1}); \quad (1)$$

where we define gate charge as $n_g = C_g V_g / 2e - n_0$, and n_0 is the offset charge due to stray charges near the box. Fig. 2(a) shows the ground state and first excited state energy bands calculated using the Hamiltonian in Eqn.(1). On account of the 2e periodicity of the system, we limit the discussion to gate charge $0 \leq n_g \leq 1$. In thermodynamic equilibrium, the actual quantity that determines

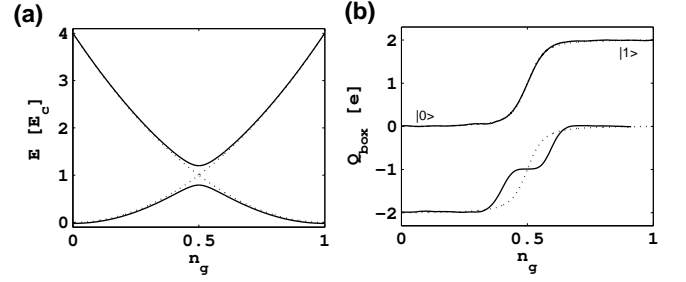


FIG. 2: (a) Ground state and first excited state energies versus n_g for $E_J = E_C = 54$ (solid line) and $E_J = 0$ (dotted line). The former was calculated using a basis with 6 charge states. (b) Coulomb staircases, Q_{box} versus n_g for sample 1 (lower solid line) in an applied parallel field $B_{jj} = 0.41$ T and sample 2 (upper solid line) with $B_{jj} = 0.45$ T. Near these magnetic fields the odd parity (short) step around $n_g = 0.5$ was smallest for sample 1 and not present for sample 2. The dotted lines (barely visible for sample 2) show the calculated Q_{box} vs n_g for these respective energies using E_J and E_C determined from spectroscopy.

the island parity is the even-odd free energy difference $\tilde{\epsilon}(T)$, which differs from ϵ due to entropic considerations and defects in the superconducting island [13]. If $\tilde{\epsilon} < E_C - E_J = 2$, the staircase acquires an extra step around $n_g = 0.5$ due to a quasiparticle, odd-parity level becoming lower in energy. Non-equilibrium quasiparticle excitations, generated by other parts of the system such as the SET, complicate the situation and can spoil the even parity ground states even if $\tilde{\epsilon} > E_C$.

Measurements were made for two different samples (referred to here as 1 and 2), however, the quality of spectroscopic and coherent oscillation data for sample 2 was degraded, partly due to the existence of a two-level fluctuator near the SCB. In the following, we concentrate on data from sample 1. Coulomb staircases were measured by slowly ramping the box gate charge (at a rate of 40 e/s), and measuring the power reflected from the RF-SET tank circuit. Examples of the measured box charge $Q_{\text{box}}(n_g)$ for each of the two samples are shown in Fig. 2b. For parallel magnetic fields B_{jj} near zero both samples exhibited 2e periodic staircases containing long and short steps. We believe the short steps are due to slow relaxation of non-equilibrium quasiparticle excitations, since the gap was experimentally determined to be $\Delta = 2.1$ K from IV curves of the SET. The size of short step was minimum for $B_{jj} \approx 0.45$ T for sample 1, growing again for $B_{jj} > 0.5$ T as expected from the BCS dependence of Δ . Sample 2 had a small window of purely even parity staircases between B_{jj} of 0.4 and 0.5 T.

The characteristic energies E_C and E_J^{\max} of the SCB can be determined directly using microwave spectroscopy [10]. When monochromatic microwaves are applied to the SCB gate, resonant peaks and dips occur in the measured Q_{box} vs n_g staircase when the microwave

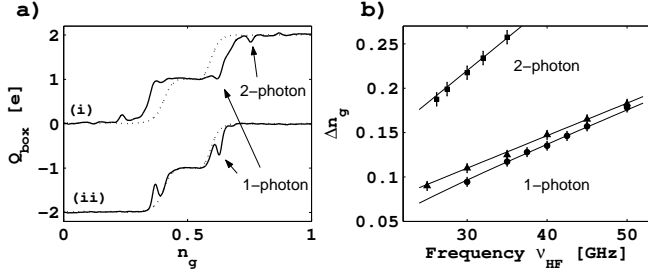


FIG. 3: (a) Measured Q_{box} vs n_g for sample 1 under applied microwaves. The dotted lines are measurements made under the same conditions in the absence of microwaves. For (i) a microwave frequency $\nu_{\text{HF}} = 36 \text{ GHz}$ and power of -36 dBm at the source with -30 dB attenuation was used. It shows resonant single photon peaks at $n_g \approx 0.37$ and $n_g \approx 0.63$. (ii) was taken using a much higher power (-6 dBm) and $\nu_{\text{HF}} = 35 \text{ GHz}$, and shows two-photon resonant peaks at $n_g \approx 0.24$ and $n_g \approx 0.76$. (b) Fitted data (sample 1) of microwave peak locations, $n_g = n_{\text{peak}} \pm 0.5$ allows a spectroscopic determination of E_C and E_J . Circles and triangles: single-photon data for maximum and minimum E_J respectively. Squares: 2-photon data.

photon energy matches the energy level splitting [Fig. 3(a)]. By increasing the microwave power, we are also able to induce two-photon transitions. Within the two-level approximation, the positions of the single-photon resonances depend on the applied frequency as $n_g = \frac{h^2}{2E_J^2} E_C^2 = 8E_C$; where we used $n_g = n_g^{\text{peak}} \pm 0.5$. (For two-photon resonances one replaces by 2.) The positions of microwave resonances for sample 1 are summarized in Fig. 3(b) and include single-photon data where $E_J = E_J^{\text{max}}$, and both single and two-photon data taken with $E_J \approx 0$. Least-squares fits to the combined data for both sample 1 [Fig. 3(b)] and sample 2 (not shown) yield $E_C = 1.64(0.04) \text{ K}$, $E_J = 0.69(0.05) \text{ K}$ for sample 1, and $E_C = 1.24(0.01) \text{ K}$, $E_J = 0.89(0.01) \text{ K}$ for sample 2.

Measurements of time-resolved, coherent oscillations of the charge on the SCB are made by slowly ramping the SCB gate charge n_g as described above, while applying fast (non-adiabatic) rectangular DC-voltage pulses of amplitude a in the form of a pulse train to the SCB gate. When n_g is far enough away from the charge degeneracy, and a such that $n_g \pm a$ places the system at the charge degeneracy, the leading and trailing edges of each pulse act as successive $\pi/2$ qubit rotations. In between, the system coherently oscillates between charge eigenstates for a time t . The trailing edge of the pulse returns the gate charge to n_g with the system in a superposition of ground and excited states corresponding to the phase of the oscillation acquired during t . After the pulse, the excited state component decays with a relaxation time T_1 . The pulses are separated by a repetition time T_R , typically greater than T_1 .

The staircase is acquired while ramping n_g on a

timescale much slower than T_R , so one measures an enhanced charge $Q_{\text{box}} = Q_{\text{box}}^{\text{on}} - Q_{\text{box}}^{\text{off}}$, that is time-averaged over the pulse train and proportional to the probability of finding the system in the excited state. Peaks in Q_{box} vs n_g will be located at gate charges n_g^{peak} such that a half-integer number of oscillations occur at gate charge $n_g^{\text{peak}} + a$ during the time t . Fig. 4(a) shows a measured staircase using such a pulse train. When one measures such staircases for varying t , then time-domain oscillations are evident in the t cross-sections of Q_{box} vs n_g . This is shown in Fig. 4(c), where we plot the time evolution at the charge degeneracy point. This data was taken using a pulse amplitude of $0.6e$ and $T_R = 91 \text{ ns}$ and hence is located along the $n_g = 0.2$ cross-section.

As T_R is increased, the pulse-induced charge contributes less to the time average. A simple calculation which ignores coherence effects remaining after a time T_R leads to $Q_{\text{box}}(T_R) = 2n_0 \frac{T_1}{T_R} (1 - e^{-T_R/T_1}) = (1 + e^{-T_R/T_1})$, where n_0 is the initial peak amplitude. One can estimate T_1 by measuring the dependence of the peak amplitude on T_R and fitting the data to this formula. This is illustrated in Fig. 4(b), where we find $T_1 = 47.2 \text{ ns}$ for $n_g = 0.2$. Previously, a considerably larger T_1 was measured in a similar sample using a spectroscopic technique [10], and found to agree with the theoretical $T_1 \approx 1 \text{ s}$ expected from quantum fluctuations of a 50 environment. The reduced T_1 observed here can be attributed to coupling to the relatively unfiltered high frequency coaxial line, in addition to unwanted coupling to other metal traces. In practice, it is difficult to estimate the actual real part of the impedance on these leads at such high transition frequencies.

Using such a pulse-train allows a measurement of the excited state probability even when the relaxation time T_1 is shorter than the inverse of the measurement bandwidth. Population averaging and mixing, however, limit the maximum observed amplitude of the Q_{box} oscillations, both in time and gate charge, to $1e$ rather than $2e$, and this occurs only for an ideal rectangular pulse and short repetition times. In Fig. 3(a) the Q_{box} oscillations in gate charge n_g have an amplitude of approximately $0.5e$. We have numerically integrated the Schrodinger equation using realistic pulses and find that the amplitude of the oscillations falls off roughly exponentially with increasing risetime, becoming approximately $0.5e$ when the risetime of the pulses is half the free oscillation period $\tau_0 = h/E_J$. These calculations agree with the measured risetime $t \approx 35 \text{ ps}$ of our pulse generator (Anritsu MP1763C) along with $\tau_0 = 75 \text{ ps}$ for our data. The initial amplitude of the time oscillations in Fig. 4(c) is further reduced from $0.5e$ due to using a repetition time somewhat longer than T_1 .

In the time oscillation data of Fig. 4(c), a non-exponential decay is clearly seen. The explanation for this could be coupling to a single (or few) modes that

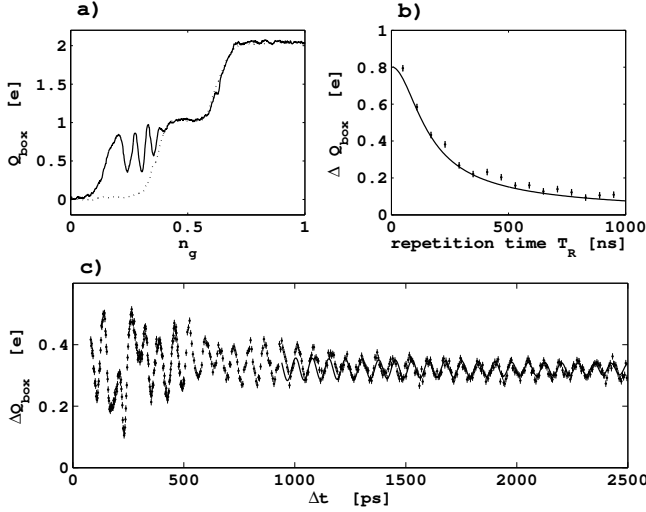


FIG. 4: (a) Measured Q_{box} vs n_g (solid line) for sample 1 with a fast pulse train applied to the SCB gate (amplitude $0.62e$, width $t = 81\text{ps}$ and repetition time $T_R = 49\text{ns}$). The dotted line is Q_{box} without the pulse train. (b) Dependence of the peak height Q_{box} on repetition time T_R for the $n_g = 0.2$ peak in (a). (c) Q_{box} versus t corresponding to evolution at the charge degeneracy (see text for parameters). The solid line is a least-squares fit to an exponentially decaying sinusoid where only data with $t > 1000\text{ps}$ is used, and gives a decay time $T_2 = 2\text{ns}$ and frequency $f_0 = 13.4\text{GHz}$.

constitute the environmental reservoir (e.g. two-level fluctuators), or possibly the SET itself. We can not presently, however, rule out instrumentale effects such as distortions of the rectangular pulses due to unwanted reflections. A fit of the data above $t = 1000\text{ps}$ to an exponentially decaying sinusoid gives a Josephson frequency $f_0 = 13.4\text{GHz}$ which agrees well with the spectroscopic measurement, however the fitted decay time of $T_2 = 2\text{ns}$ has a large uncertainty ($\sim 2\text{ns}$) for the upper limit, due to the limited range of data. The coherence time found by Vion et al.[2] is much larger than that found in our measurements although their initial oscillation amplitude is much smaller. The apparent decoherence time of $\sim 2\text{ns}$ observed here could be due to a finite lifetime of the even-parity state. The coherent oscillations shown in Fig. 4 are visible outside the odd-parity step, even though the pulse takes the gate charge inside the odd-parity step. In any case, this means the lifetime of the even-parity states inside the odd-parity region must be greater than $\sim 2\text{ns}$:

The most noted source of decoherence in charge qubits, however, is due to $1/f$ charge noise. Vion et al.[2] demonstrate that this contribution can be minimized by working at an optimal point that is the conjunction of the charge degeneracy with the maximum of E_J vs ϕ for the box SQUID loop. To take advantage of this reduction of charge noise, the system must be kept firmly at the optimal point. This is difficult using fast rectangular pulses since the evolution at the degeneracy occurs at the top of

the pulse and therefore requires a very high pulse fidelity. Also the effective charge noise at the optimal point increases with increasing E_C/E_J ratio as $(E_C/E_J)^2$. This suggests our qubit is an order of magnitude more sensitive to charge fluctuations than that reported in Vion et al. Another source of decoherence for the qubit described here includes backaction of the SET measuring device.

In conclusion, we have fabricated and measured a solid state qubit based upon a SCB combined with a RF-SET readout system. Fast DC pulses were used to coherently manipulate the qubit, and time-coherent oscillations of the charge were observed with amplitudes of $0.5e$ understood as coming from the finite risetime of the pulses. The oscillations exhibit a non-exponential decay, especially below 1ns , and persist to a few ns. Due to a relatively short T_1 , continuous measurement of the SCB was employed. Single-shot readout should be possible if T_1 can be increased so that the decay of the excited state is slower than the bandwidth of the RF-SET.

We would like to acknowledge fruitful discussions with K. Lehnert, A. Wallra, G. Johansson, A. Kack, G. Wendin and Y. Nakamura. The samples were made at the MC2, Chalmers. The work was supported by the Swedish SSF and VR, by the Wallenberg and Goran Gustafsson foundations, by the EU under the IST-SQUBIT programme, and by the Army Research Office under Contract No. DAAAD19-02-1-0045.

tim@fy.chalmers.se

- [1] Y. Nakamura, Y. A. Pashkin, and J. S. Tsai, Nature 398, 786 (1999).
- [2] D. Vion, A. Aassime, A. Cottet, P. Joyez, H. Pothier, C. Urbina, D. Esteve, and M. H. Devoret, Science 296, 886 (2002).
- [3] C. H. van der Wal et al., Science 290, 773 (2000).
- [4] I. Chiorescu, Y. Nakamura, C. J. P. M. Harmans, J. E. Mooij, Science (2003).
- [5] Y. Yu, S. Han, X. Chu, S.-I. Chu, and Y. Wang, Science 296, 889 (2002).
- [6] J. M. Martinis, S. Nam, J. Aumentado, and C. Urbina, Phys. Rev. Lett. 89, 117901-1 (2002).
- [7] R. J. Schoelkopf, P. Wang, A. A. Kozhevnikov, P. Delsing, and D. E. Prober, Science 280, 1238 (1998).
- [8] A. Aassime, D. Gunnarsson, K. Bladh, and P. Delsing, Appl. Phys. Lett. 79, 4031 (2001).
- [9] A. Aassime, G. Johansson, G. Wendin, H. Schoelkopf, and P. Delsing, Phys. Rev. Lett. 86, 3376 (2001).
- [10] K. W. Lehnert, K. Bladh, L. F. Spietz, D. Gunnarsson, D. I. Schuster, P. Delsing, and R. J. Schoelkopf, Phys. Rev. Lett. 90, 027002 (2003).
- [11] K. Bladh et al., Physica Scripta T 102, 167 (2002).
- [12] A. A. Clerk, S. M. Girvin, A. K. Nguyen, and A. D. Stone, Phys. Rev. Lett. 89, 176804-1 (2002).
- [13] P. Lafarge, P. Joyez, D. Esteve, C. Urbina, M. H. Devoret, Nature 365, 6445 (1993).